

Anaerobic Degradation of Phthalate Isomers by Methanogenic Consortia

ROBERT KLEEREBEZEM,* LOOK W. HULSHOFF POL, AND GATZE LETTINGA

Subdepartment of Environmental Technology, Department of Agricultural, Environmental, and Systems Technology, Wageningen Agricultural University, 6703 HD Wageningen, The Netherlands

Received 8 June 1998/Accepted 15 December 1998

Three methanogenic enrichment cultures, grown on *ortho*-phthalate, *iso*-phthalate, or terephthalate were obtained from digested sewage sludge or methanogenic granular sludge. Cultures grown on one of the phthalate isomers were not capable of degrading the other phthalate isomers. All three cultures had the ability to degrade benzoate. Maximum specific growth rates ($\mu_{\text{S}}^{\text{max}}$) and biomass yields ($Y_{\text{X}_{\text{totS}}}$) of the mixed cultures were determined by using both the phthalate isomers and benzoate as substrates. Comparable values for these parameters were found for all three cultures. Values for $\mu_{\text{S}}^{\text{max}}$ and $Y_{\text{X}_{\text{totS}}}$ were higher for growth on benzoate compared to the phthalate isomers. Based on measured and estimated values for the microbial yield of the methanogens in the mixed culture, specific yields for the phthalate and benzoate fermenting organisms were calculated. A kinetic model, involving three microbial species, was developed to predict intermediate acetate and hydrogen accumulation and the final production of methane. Values for the ratio of the concentrations of methanogenic organisms, versus the phthalate isomer and benzoate fermenting organisms, and apparent half-saturation constants (K_{S}) for the methanogens were calculated. By using this combination of measured and estimated parameter values, a reasonable description of intermediate accumulation and methane formation was obtained, with the initial concentration of phthalate fermenting organisms being the only variable. The energetic efficiency for growth of the fermenting organisms on the phthalate isomers was calculated to be significantly smaller than for growth on benzoate.

All three phthalic acid isomers (*ortho*, *meta*, and *para* benzene dicarboxylic acid) are produced in massive amounts around the world and are primarily anthropogenic compounds. They are used in the chemical production of a wide range of plastics. Diesters of *ortho*-phthalic acid are mainly used as a plasticizer in the production of polyvinyl chloride (10). *para*-Phthalic acid (terephthalic acid) and the corresponding dimethyl ester are used in the production of polyester fibers and polyethylene terephthalate. This latter compound is well known for its application in bottles for carbonated drinks. *meta*-Benzene dicarboxylic acid (isophthalic acid) is produced in smaller amounts than its *ortho*- and *para*-oriented isomers and is used in the production of specialty chemicals.

Introduction of phthalic acid isomers into the environment may occur through leaching from plastics (10). In addition to this diffuse source of environmental pollution with phthalic acids, large point sources are generated during production of phthalate isomers from their corresponding xylenes (2). Both liquid and solid wastestreams, generated during production of the phthalate isomers, contain high concentrations of these aromatic acids. Furthermore, heavily contaminated soil with high concentrations of phthalic acid isomers can be found around chemical factories (20).

Microbial activity is the principal method for the removal of phthalic acid isomers and their corresponding esters from the environment. The metabolic pathway for anaerobic degradation of phthalic acid isomers in a denitrifying *Pseudomonas* sp. in-

volves initial activation of *ortho*-phthalate by coenzyme A (CoA), probably followed by decarboxylation resulting in the formation of benzoyl CoA (21, 22, 30). No experimental evidence is available about the exact location of the decarboxylation in the degradation pathway, but the current view is that benzoyl-CoA is the only central intermediate in the anaerobic mineralization of a large range of aromatic compounds (besides aromatic compounds with at least two phenolic functional groups). Degradation of benzoyl-CoA proceeds through initial reduction of the aromatic ring, followed by ring cleavage (9, 26). Hardly any information is available about the anaerobic mineralization of phthalate isomers under sulfate reducing or methanogenic conditions. It has been suggested that methanogenic degradation of *ortho*-phthalate proceeds analogously to degradation under denitrifying conditions because methanogenic enrichment cultures grown on *ortho*-phthalate had the ability to degrade benzoate (26).

In methanogenic environments, complex organic matter (including aromatic compounds) is converted into a mixture of methane and carbon dioxide in a complex network of various metabolic groups of bacteria. Bacteria in these consortia depend entirely on each other to perform the metabolic conversions observed (25, 28) and are therefore referred to as syntrophic consortia. In these syntrophic consortia, fermentative bacteria convert complex organic matter into a mixture of acetate and hydrogen or formate, which are substrates for methanogenic bacteria. Fermentative conversions of substrates are often energetically unfavorable under standard conditions ($\Delta G^{\circ} > 0$), implying the need for continuous removal of the fermentative products by methanogens.

In this study three methanogenic enrichment cultures degrading either *ortho*-phthalate, isophthalate, or terephthalate are described. Emphasis is put on the kinetics of mineralization of the phthalate isomers. A method is described to calcu-

* Corresponding author. Mailing address: Wageningen Agricultural University, Department of Agricultural, Environmental and Systems Technology, Subdepartment of Environmental Technology, "Biotechnion" Bomenweg 2, 6703 HD Wageningen, The Netherlands. Phone: (31-317) 483798. Fax: (31-317) 482108. E-mail: robbert.kleerebezem@algemeen.mt.wau.nl.

TABLE 1. Chemical reaction equations for the individual steps in mineralization of phthalate isomers and benzoate and the standard Gibbs free-energy changes during the conversions, corrected for a temperature of 37°C

Reaction no.	Reaction	Equation	ΔG^0 , 37°C (kJ · reaction ⁻¹)
1	Phthalate fermentation	$C_8H_4O_4^{2-} + 8H_2O \rightarrow 3C_2H_3O_2^- + 3H^+ + 3H_2 + 2HCO_3^-$	38.9 ^a
2	Benzoate fermentation	$C_7H_5O_2^- + 7H_2O \rightarrow 3C_2H_3O_2^- + 3H^+ + 3H_2 + HCO_3^-$	59.6
3	Hydrogenotrophic methanogenesis	$0.75HCO_3^- + 0.75H^+ + 3H_2 \rightarrow 0.75CH_4 + 2.25H_2O$	-98.4
4	Acetoclastic methanogenesis	$3C_2H_3O_2^- + 3H^+ \rightarrow 3CH_4 + 3CO_2$	-97.8
5	Mineralization of phthalate	$C_8H_4O_4^{2-} + 6.5H_2O \rightarrow 3.75CH_4 + 2HCO_3^- + 2.25CO_2$	-157.3
6	Mineralization of benzoate	$C_7H_5O_2^- + 5.5H_2O \rightarrow 3.75CH_4 + HCO_3^- + 2.25CO_2$	-136.6

^a The value represents the calculated ΔG^0 for isophthalate and terephthalate fermentation; the value for *ortho*-phthalate fermentation is estimated to be 34.9 kJ · reaction⁻¹. Applied ΔG_f^0 values for *ortho*-phthalate, isophthalate, and terephthalate were -548.6, -552.6, and -552.7, respectively (5).

late the kinetic parameters of the individual trophic groups involved in mineralization of the aromatic substrates. The specific role of benzoate in the anaerobic degradation of terephthalate is presented in a separate study (14).

MATERIALS AND METHODS

Source of the biomass and enrichment procedure. Biodegradability experiments were performed with three different types of biomass and a set of aromatic compounds that are present in phthalic acid isomer production wastewaters (13). Sludge types used for these experiments were digested sewage sludge and two types of granular sludge from full-scale upflow anaerobic sludge bed (UASB) reactors. The initial concentrations of the phthalate isomers were 2.1 mM. When, after a lag phase ranging from 15 to 150 days, mineralization of the phthalate isomers was observed, the substrate was replenished to a concentration of 6 mM. Substrate dosage was repeated until a phthalate isomer degradation rate of approximately 1 mM · day⁻¹ was reached. At this point 20% of the culture liquid was transferred into pre-reduced fresh medium containing 6 to 12 mM phthalate isomer. Cultivation was performed in 300-ml serum bottles sealed with butyl rubber septa by using a liquid volume of 70 ml. Serum bottles were incubated statically at 37°C in the dark. To monitor degradation of the phthalate isomers, the methane concentration in the headspace of the serum bottles was measured at least twice a week. This procedure was used for more than 18 months in order to obtain stable and highly enriched cultures. Best growth on *ortho*-phthalate was obtained with the culture initially seeded with granular sludge from a UASB reactor treating wastewater from a paper factory, while cultivation on isophthalate proceeded most rapidly with cultures initially seeded with digested sewage sludge. These two enrichment cultures were therefore used for the experiments described here.

The inoculum of the terephthalate degrading enrichment culture was obtained from a laboratory-scale anaerobic hybrid reactor. Hybrid reactors are upflow reactors equipped with carrier material in the top of the reactor instead of the three-phase separator used in UASB reactors. The hybrid reactor had been in continuous operation for a period of 12 months with terephthalate as the sole carbon and energy source. The specific terephthalate conversion rate of the biomass grown in this reactor was approximately 1.7 mmol · (g · day)⁻¹. Similar cultivation methods were used as described for the *ortho*-phthalate and isophthalate degrading cultures for more than 1 year before the experiments described here were carried out.

Medium and substrate preparation. The basal medium used in the experiments contained the following (in mg · liter of liquid volume⁻¹): NaHCO₃, 3,000; NH₄Cl, 280; K₂HPO₄, 250; CaCl₂ · 2H₂O, 10; yeast extract, 18; and 1 ml of a trace element stock solution according to the composition described by Huser et al. (12). Stock solutions of disodium *ortho*-phthalate, isophthalate, and terephthalate were prepared in demineralized water.

Experimental procedure. Experiments were performed in 300- or 120-ml serum bottles with liquid volumes of 70 or 25 ml, respectively. Medium and substrate were added to the serum bottles. The bottles were sealed with butyl rubber septa and aluminum screw or crimp caps, and the headspace was flushed with a mixture of N₂ and CO₂ (70:30 [vol/vol]). After flushing, Na₂S · 7-9H₂O was added from a concentrated stock solution to obtain a final concentration of 150 mg · liter⁻¹. Serum bottles were preincubated at 37 ± 1°C in an orbital-motion shaker prior to inoculation by syringe. Liquid samples (1 ml) were withdrawn from the serum bottles for component analyses. Measured methane concentrations in the headspaces of the bottles were corrected for the volumes of samples removed.

Analytical procedures. The methane content of the headspace was determined by gas chromatography (Hewlett Packard 438/S). Samples (100 µl) were injected by using a gas-lock syringe (Dynatech, Baton Rouge, La.). A stainless-steel column (2 m by 2 mm) packed with Poropak Q (80 to 100 mesh) was used. Nitrogen was used as a carrier gas. The temperatures of the column, injection port, and flame ionization detector were 60, 200, and 220°C, respectively.

The concentration of water-soluble aromatic acids was determined by high-pressure liquid chromatography (HPLC). Centrifuged liquid samples (3 min at

10,000 × g) were diluted to concentrations smaller than 50 mg · liter⁻¹ by using a Meyvis Dilutor (type no. 401), and a volume of 10 µl was injected by using an autosampler (Marathon). Separation of the aromatic acids was obtained by using a Chromospher 5C18 column (100 by 3 mm). The solvent used as a carrier was a mixture of methanol and a 1% acetic acid solution in water in a 40/60 ratio. The applied flow rate amounted 0.3 ml · min⁻¹. The separated components were detected by a UV detector (Spectroflow 773) at a wavelength of 230 nm. Typical retention times for *ortho*-phthalate, terephthalate, isophthalate, and benzoate were 2.8, 3.6, 4.1, and 6.8 min, respectively. Chromatograms were stored and integrated by using the software package Minichrom.

The concentration and composition of volatile fatty acids in the medium were determined with a gas chromatograph (Hewlett Packard 5890A). A glass column (2 m by 4 mm) packed with Supelcoport (100 to 200 mesh), coated with 10% Fluorad FC431, was used. The temperatures of the column, injection port, and flame ionization detector were 130, 200, and 280°C, respectively. Nitrogen gas saturated with formic acid was used as a carrier gas at a flow rate of 50 ml · min⁻¹. Prior to analysis, the samples were diluted and fixed with a formic acid solution (3% [vol/vol]). After formic acid addition aromatic acids precipitate, and samples had to be centrifuged (3 min, 10,000 × g).

Hydrogen was determined by gas chromatography (Hewlett Packard 5890). The gas chromatograph was equipped with a stainless-steel column (1.5 m by 6.4 mm) packed with molecular sieve 25H (60 to 80 mesh). The temperatures of the column, injection port, and thermal conductivity detector were 40, 110, and 125°C, respectively. Argon was used as a carrier gas at a flow rate of 25 ml · min⁻¹.

Determination of kinetic parameters. The total biomass yield of the mixed cultures growing on the phthalate isomers and benzoate was determined in batch experiments. A known amount of biomass was transferred into fresh medium containing a high concentration of substrate (10 to 12 mM for benzoate and the phthalate isomers). After complete mineralization of the substrate, the concentration of volatile solids was determined and the biomass yield was calculated by relating the increase of the biomass concentration to the amount of substrate degraded. In case of degradation of a complex substrate by a syntrophic culture, the sum of the yield factors of all the species participating in the degradation is measured. Consequently, the measured yield is referred to as $Y_{X_{tot}}$ (g · mol⁻¹ · S⁻¹). For determination of the microbial yield on acetate ($Y_{X_{AcM(C_2)}}$), several portions of 5 mM acetate were supplied to avoid substrate inhibition.

The maximum specific growth rate (μ_s^{max} , day⁻¹) of the cultures was calculated from the exponential part of substrate depletion and/or product formation curves. In case of zero-order kinetics ($C_s \gg K_s$), Monod-based equations for substrate depletion and product formation can be integrated and the following equations apply (neglecting maintenance and/or decay):

$$C_s(t) = C_s(0) + \frac{C_x(0)}{Y_{X_{tot}S}} \cdot (1 - e^{\mu_s^{max} \cdot t}) \quad (1)$$

$$C_p(t) = C_p(0) - f_{SP} \cdot (1 - \eta_{X_{tot}S}) \cdot \frac{C_x(0)}{Y_{X_{tot}S}} \cdot (1 - e^{\mu_s^{max} \cdot t}) \quad (2)$$

where f_{SP} stands for the number of moles of product, produced per mole of substrate (mol · P · mol⁻¹ · S⁻¹) according to the stoichiometry of the reaction (Table 1), and $\eta_{X_{tot}S}$ is the electron yield as can be calculated from the measured yield according to equation A-4 (see Appendix). By using measured values for the microbial yield and measured substrate concentrations (C_s , mol · liter⁻¹) and/or product concentrations (C_p , mol · liter⁻¹) as a function of time, the initial biomass concentration [$C_x(0)$, g · liter⁻¹] and μ_s^{max} can be estimated with an optimization procedure as available in most spreadsheet programs. Optimization was based on minimizing the absolute error between measured and calculated values for C_s and C_p .

Calculation of kinetic parameters. In order to describe intermediate accumulation and final methane production during growth of the mixed cultures on the phthalate isomers and benzoate, a mathematical model was derived (see Appendix). Nonmeasured parameter values that were required as input for the model were estimated by using the procedures described below.

The biomass yield of the organisms responsible for fermentation of the phthalate isomers and benzoate ($Y_{X_{FermS}}$) was calculated from the (measured) total

TABLE 2. Maximum specific growth rate (μ_S^{\max}) and total biomass yield ($Y_{X_{\text{tot}},S}$) for three phthalate-isomer-degrading enrichment cultures, grown on the phthalate isomers, benzoate, or acetate^a

Culture	Substrate	$Y_{X_{\text{tot}},S}$ (g [dry wt] · mol ⁻¹)	μ_S^{\max} (day ⁻¹)
Isophthalate	Isophthalate	8.5 (0.8)	0.092 (0.012)
	Benzoate	11.5 (0.6)	0.130 (0.020)
	Acetate	0.97 (0.09)	0.131 (0.014)
<i>ortho</i> -Phthalate	<i>ortho</i> -Phthalate	8.2 (1.2)	0.087 (0.007)
	Benzoate	12.8 (0.5)	0.216 (0.009)
	Acetate	1.01 (0.15)	0.100 (0.013)
Terephthalate	Terephthalate	8.6 (0.5)	0.094 (0.007)
	Benzoate	12.9 (1.2)	0.180 (0.011)
	Acetate	1.23 (0.11)	0.120 (0.009)

^a Values in parentheses represent standard deviations of the measured values. Values are the average of at least three separate measurements.

biomass yields ($Y_{X_{\text{tot}},S}$) and the biomass yields of the acetoclastic and hydrogenotrophic methanogens ($Y_{X_{\text{AcM}}}$ and $Y_{X_{\text{HyM}}}$) according to the following equation:

$$Y_{X_{\text{FermPA}}} = Y_{X_{\text{totPA}}} - f_{\text{PAC2}} \cdot (1 - \eta_{X_{\text{FermPA}}}) \cdot Y_{X_{\text{AcM}}} - f_{\text{PAH2}} \cdot (1 - X_{\text{FermPA}}) \cdot Y_{X_{\text{HyM}}} \quad (3)$$

where f_{PAC2} and f_{PAH2} are, respectively, the number of moles of acetate and of hydrogen formed per mole of phthalate isomer (mol-C2/H2 · mol-PA⁻¹) according to the chemical reaction equation for phthalate fermentation (Table 1, reaction 1), and $\eta_{X_{\text{FermPA}}}$ is the electron yield of the phthalate isomer fermenting culture (e-mol- X_{FermPA} · e-mol-PA⁻¹). Substitution of equation A-4 (Appendix) into equation 1 allows for direct calculation of the biomass yield for the fermenting bacteria.

Since during growth on the phthalate isomers the intermediate concentrations of acetate and hydrogen were found to be relatively constant (dC_{C2}/dt and dC_{H2}/dt equal 0; Fig. A1), the actual specific growth rates of the different species in the mixed culture must be equal (23). Definition of this boundary condition allows for calculation of the concentration ratio of the acetoclastic methanogens relative to the fermenting organisms according to the following equation:

$$\frac{C_{X_{\text{Ferm}}}}{C_{X_{\text{AcM}}}} = \frac{Y_{X_{\text{FermPA}}}}{f_{\text{PAC2}} \cdot (1 - \eta_{X_{\text{FermPA}}}) \cdot Y_{X_{\text{AcM}}}} \quad (4)$$

From the average concentrations of acetate and hydrogen measured during exponential growth on the phthalate isomers (see Table 3) and the observation that these concentrations remained constant during growth on the phthalate isomers, the apparent half-saturation constants for acetate and hydrogen (K_{C2} and K_{H2}) can be estimated. At phthalate concentrations significantly higher than the half-saturation constant for phthalate fermentation ($K_{\text{P,PA}}$), the following equation enables calculation of K_{C2} :

$$K_{\text{C2}} = \frac{C_{\text{C2}}^{\text{avg}}}{\frac{q_{X_{\text{FermPA}}}^{\text{max}} \cdot f_{\text{PAC2}} \cdot (1 - \eta_{X_{\text{FermPA}}}) \cdot X_{\text{Ferm}}}{q_{X_{\text{AcM}}}^{\text{max}} \cdot X_{\text{AcM}}} - C_{\text{C2}}^{\text{avg}}} \quad (5)$$

Expressions equivalent to equations 4 and 5 were used for calculation of $C_{X_{\text{Ferm}}}/C_{X_{\text{HyM}}}$ and K_{H2} .

Gibbs free-energy changes. Standard Gibbs free-energy changes for the individual steps in an anaerobic mineralization of the phthalate isomers and benzoate were calculated according to the method of Thauer et al. (31) (Table 1). ΔG_r^0 values for the phthalate isomers were calculated from benzoate by using the group contribution method described by Dimroth (5). ΔG_r^0 values were corrected for a temperature of 37°C by using the Van't Hoff equation (4).

Microscopical observation. The cultures were routinely observed by using a phase-contrast microscope. Cultures grown on *ortho*-phthalate and isophthalate were prepared for scanning electron microscopy. Samples (10 ml) were filtered into 1-ml observation chambers. The observation chambers were closed and fixed with 2.5% glutaraldehyde. After fixation, samples were stored overnight in a 0.5% osmium tetroxide solution in a buffer of sodium cacodylate (0.1 M, pH 7.1). After three rinses with demineralized water, samples were dehydrated stepwise with ethanol. Samples were mounted on stubs with carbon cement, critical point dried with CO₂, and sputter coated with 3 nm of platinum. The coated specimens were observed in a Jeol JSM 6300F scanning microscope at 5 to 8 kV.

RESULTS

Enrichment cultures. Three stable enrichment cultures with the ability to degrade either *ortho*-phthalate, isophthalate, or terephthalate were obtained through numerous transfers into fresh medium throughout a period of more than 1 year. Multiple doses of substrate (6 to 12 mM phthalate isomer) were necessary to obtain high conversion rates. Once the conversion rate amounted to approximately 1 mM · day⁻¹, 20% of the culture was transferred into fresh medium. No stable growth was obtained when (i) smaller amounts of the cultures were transferred or when (ii) the cultures were transferred when rates were significantly lower. Moreover, when transferring the cultures after complete depletion of the substrate, long lag phases and nonexponential growth were observed. These observations were studied in more detail by using the terephthalate-grown enrichment culture, and the results obtained are described elsewhere (14). Due to their low growth rate (Table 2), the cultures could be transferred approximately once a month. A typical example of the methane production profile found during several transfers of the isophthalate-grown culture into fresh medium is shown in Fig. 1.

Cultures grown on one of the phthalate isomers were not able to degrade either of the other two phthalate isomers, suggesting that specific organisms are responsible for the degradation of each of the phthalate isomers. All three cultures were able to degrade benzoate without a lag period at rates comparable to the phthalate isomer degradation rates.

During exponential growth on the phthalate isomers, only small amounts of acetate and hydrogen were found (approximately 1 to 4 mM and 3 to 5 Pa, respectively), indicating tight syntrophic coupling between the fermenting organisms and the methanogens (Fig. 2). Intermediate accumulation of benzoate was only observed in the *ortho*-phthalate-grown culture, but the measured concentrations were very low (1 to 3 μ M). No other intermediates were detected during exponential growth on the phthalate isomers.

Addition of Na₂SO₄ as an exogenous electron acceptor (final concentration, 5 mM) did not affect the phthalate isomer conversion rate in any of the three cultures. The addition of NaNO₃ (final concentration, 5 mM) resulted in complete inhibition of the degradation of the phthalate isomers.

Kinetic parameters. The calculated values for the maximum specific growth rate (μ_S^{\max}) and the total yield ($Y_{X_{\text{tot}},S}$) of the

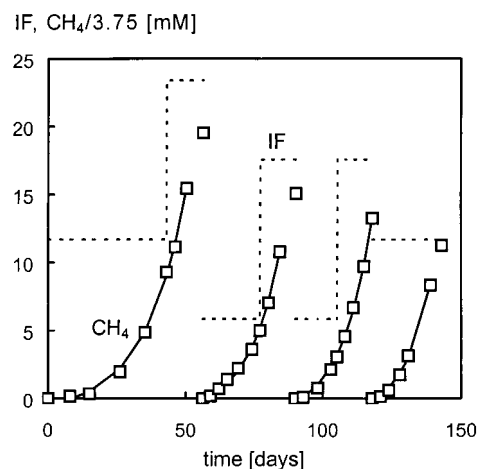


FIG. 1. Calculated (solid lines) and measured (\square) methane concentrations (CH_4) and substrate levels (dashed lines) during several transfers of the isophthalate (IF)-grown culture.

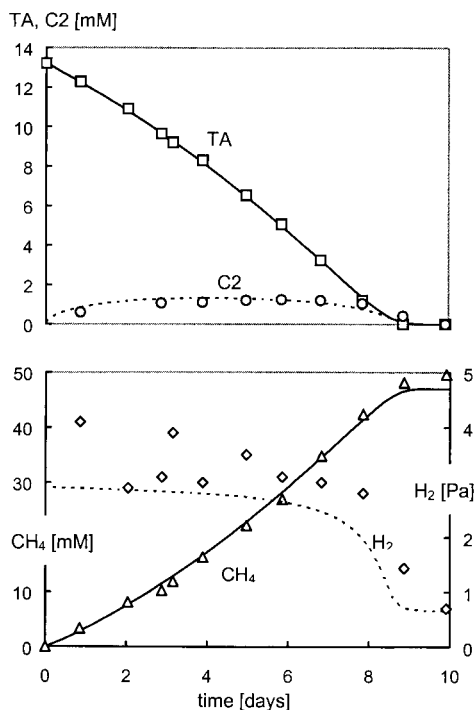


FIG. 2. Terephthalate (TA, \square) degradation and intermediate accumulation of acetate (C2, \circ) and hydrogen (H_2 , \diamond) and final production of methane (CH_4 , \triangle). Markers correspond to measured concentrations and lines were drawn by using the mathematical model described in the Appendix.

three cultures are summarized in Table 2. Values for these parameters were determined with the three phthalate isomers, with benzoate and acetate as substrates. Both parameters were measured in exponentially growing batch cultures.

From the data presented in Table 2 it can be seen that the differences in μ_S^{\max} and $Y_{X_{tot}S}$ among the three cultures grown on either phthalate, isophthalate, or terephthalate are small. For all enrichment cultures, μ_S^{\max} and $Y_{X_{tot}S}$ are significantly smaller for the phthalate isomer than for benzoate.

When the maximum specific growth rates on acetate and the phthalate isomers are compared, it can be seen that higher values were found for growth on acetate. These data suggest that only limited amounts of acetate will accumulate during degradation of the phthalate isomers. This was confirmed by the low concentrations of acetate, measured during exponential growth on the phthalate isomers (1 to 4 mM), as shown in Fig. 2 for growth on terephthalate.

The situation is different for growth on benzoate. The calculated maximum specific growth rates of the cultures grown on benzoate are either comparable (isophthalate and terephthalate) or significantly higher (*ortho*-phthalate) than the maximum specific growth rates determined with acetate. These parameter values indicate that during incubation of the *ortho*-phthalate-grown culture with benzoate, large amounts of acetate will accumulate. Smaller amounts of acetate are predicted to accumulate in the isophthalate- and terephthalate-grown cultures when incubated with benzoate. These indications were confirmed by measured acetate concentrations during benzoate degradation, as shown in Fig. 3.

Product formation during degradation of the phthalate isomers when incubated with BES. In order to study product formation of the fermenting organisms, the cultures were incubated with the phthalate isomers and 10 mM bromoethanesulfonate (BES), a specific inhibitor of methanogenesis. From

the results shown in Fig. 4 it can be seen that trace amounts of benzoate accumulated during incubation with BES of a terephthalate-grown culture. No benzoate was detected in exponentially growing cultures, except for the *ortho*-phthalate-grown culture, where up to 3 μ M benzoate was found.

The methanogenic substrates acetate and hydrogen accumulated to concentrations significantly higher than those observed in exponentially growing cultures. According to the stoichiometry of the fermentation of the phthalate isomers (Table 1, reaction 1), equimolar amounts of acetate and hydrogen should accumulate during incubation with BES. However, the results show that much higher concentrations of acetate accumulate. Two reasons can be distinguished to explain this observation: (i) small amounts of methane were formed during

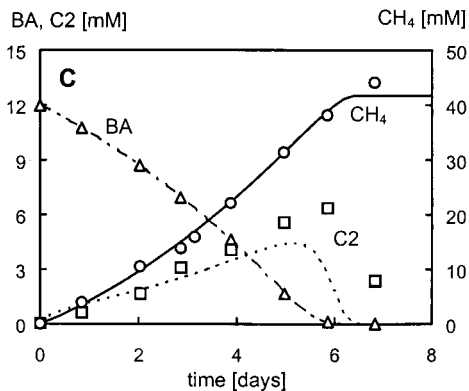
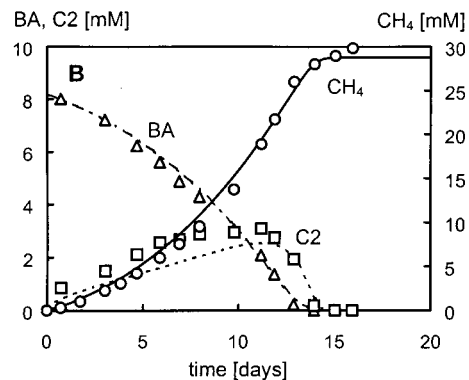
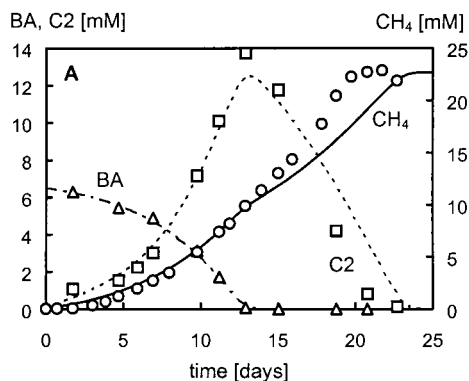


FIG. 3. Benzoate (BA, \triangle) degradation and concomitant acetate (C2, \square) accumulation and methane (CH_4 , \circ) formation in *ortho*-phthalate (A)-, isophthalate (B)-, and terephthalate (C)-grown cultures. Markers correspond to measured concentrations, and lines were calculated by using the mathematical model described in the Appendix.

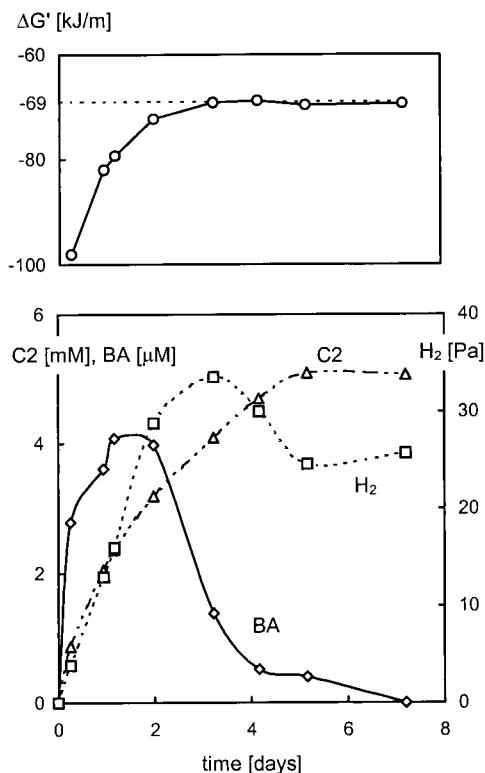


FIG. 4. Accumulation of acetate (C2, Δ), benzoate (BA, \diamond), and molecular hydrogen (H₂, \square) during incubation of the terephthalate-grown culture with terephthalate and 20 mM BES (bottom graph). The actual Gibbs free energy for terephthalate fermentation (Table 1, reaction 1) is indicated in the top graph.

the initial 2 days of incubation, suggesting incomplete initial inhibition of methanogenesis from hydrogen by BES, and (ii) the formation of another reduced product besides molecular hydrogen was observed. This product was identified as cyclohexanecarboxylate by gas chromatography.

Based on the measured concentrations of the phthalate isomer, acetate, and hydrogen, the actual Gibbs free energy ($\Delta G'$) for fermentation of the phthalate isomers (Table 1, reaction 1) can be calculated. From Fig. 4 it can be seen that fermentation of terephthalate stopped at $\Delta G'$ values exceeding $-69 \text{ kJ} \cdot (\text{mol-terephthalate})^{-1}$. As for the fermentation of terephthalate, the degradation of *ortho*-phthalate and *isophthalate* stopped when $\Delta G'$ exceeded approximately $-65 \text{ kJ} \cdot (\text{mol-phthalate isomer})^{-1}$.

Microscopical observation. All three phthalate isomer-grown cultures formed dense flocs of 0.5 to 2 mm in statically incubated serum bottles. *Methanosaeta*-like organisms were identified as the predominant acetoclastic methanogen in all three cultures.

In the *ortho*-phthalate-grown culture (Fig. 5A), two dominant types of organisms were observed other than the *Methanosaeta*-like organisms (arrow 1): short fat rods (0.6 to 0.8 by 1 to 2 μm) with rounded ends (arrow 2) and very small rods (0.3 by 1.0 to 1.2 μm) (arrow 3). The fat rods were found in large amounts and are presumed to be responsible for the fermentation of *ortho*-phthalate. The very small rods were embedded in extracellular material and always close to the short fat rods and may be hydrogenotrophic methanogens belonging to the genus *Methanobacterium*.

The *isophthalate*-grown culture (Fig. 5B) was less well defined than the *ortho*-phthalate-grown culture, which may partly

be the result of the low conversion rates observed in this culture at the moment samples were drawn for electron microscopy. Dense clusters of different types of organisms, embedded in extracellular material, were observed in a loose matrix of *Methanosaeta*-like organisms.

The terephthalate-grown culture was only examined with a light microscope (not shown) and spore-forming rods of 3 to 4 μm were observed besides *Methanosaeta*- and *Methanospirillum*-like organisms. The spore-forming rods were probably involved in the fermentation of terephthalate.

DISCUSSION

General observations. At least three different species of bacteria are involved in the methanogenic degradation of the phthalate isomers: fermentative organisms that convert the phthalate isomers to a mixture of acetate and hydrogen (Table 1, reaction 1), acetoclastic methanogens that convert acetate into a mixture of methane and bicarbonate (Table 1, reaction 4), and hydrogenotrophic methanogens that reduce bicarbonate with hydrogen under formation of methane (Table 1,

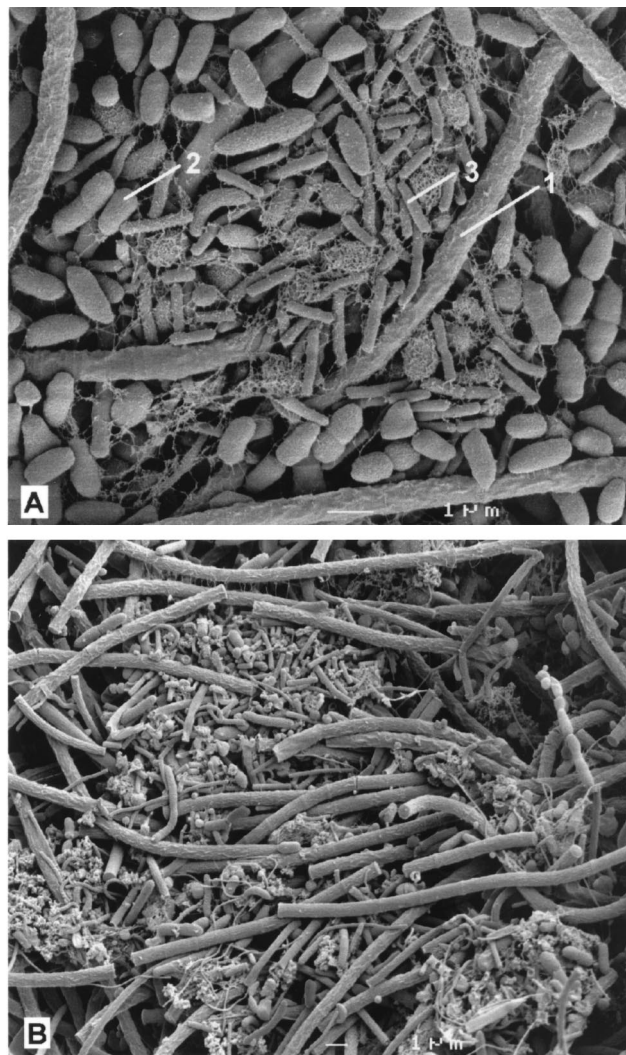


FIG. 5. Scanning electron micrographs of the methanogenic enrichment cultures grown on *ortho*-phthalate (A) and *isophthalate* (B). The numbers are explained in the text.

TABLE 3. Specific biomass yields, specific phthalate- and benzoate-fermenting activities, and the specific biomass yield values normalized to an energy quantum of $70 \text{ kJ} \cdot \text{mol}^{-1}$ of the fermentative organisms in the three mixed cultures grown on benzoate or the phthalate isomers

Culture	Substrate	Y_{XFermS} (g [dry wt] · mol ⁻¹)	$q_{\text{XFermS}}^{\text{max}}$ ^a (mol-S · [g (dry wt) · day] ⁻¹)	Acetate ^b (mM)	H ₂ ^b (Pa)	ΔG^{c} (kJ · mol-S ⁻¹)	$Y_{\text{XFerm}\Delta G}^{\text{d}}$ (g [dry wt] · 70 kJ ⁻¹)
Isophthalate	Isophthalate	4.7	0.019	1.6	3.5	-92.4	3.6
	Benzoate	7.8	0.017	2.5	6.0	-56.0	9.7
Phthalate	Phthalate	4.3	0.020	4.0	4.0	-88.5	3.4
	Benzoate	9.0	0.024	10.0	6.0	-45.2	13.9
Terephthalate	Terephthalate	4.0	0.023	1.3	3.0	-95.4	3.0
	Benzoate	8.4	0.021	2.5	4.0	-59.1	10.0

^a The maximum specific conversion rate was calculated according as follows: $q_{\text{XFermS}}^{\text{max}} = \mu_{\text{S}}^{\text{max}} \cdot Y_{\text{XFermS}}^{-1}$.

^b The acetate and hydrogen concentrations represent average concentrations, as measured during exponential growth of the cultures.

^c Values for the actual Gibbs free-energy change for fermentation of the phthalate isomers (reaction 1, Table 1) and benzoate (reaction 2, Table 1), calculated with a concentration of 4 mM for the phthalate isomers and benzoate and a bicarbonate concentration of 40 mM.

^d Measured biomass yields (see Table 2) normalized to an energy quantum of $70 \text{ kJ} \cdot (\text{mol-S})^{-1}$.

reaction 3). Conversion of the phthalate isomers into acetate and hydrogen is energetically unfavorable under standard conditions ($\Delta G^{\text{O}'} = 38.6 \text{ kJ} \cdot \text{mol-phthalate}^{-1}$), suggesting that the phthalate-isomer-fermenting cultures strictly depend on the presence of acetoclastic and hydrogenotrophic methanogens in the mixed culture to maintain sufficiently low intermediate concentrations of acetate and hydrogen. Methanogens depend on the phthalate-isomer-fermenting bacteria for generation of their substrates. Due to their mutual dependency, the mixed cultures can be designated as syntrophic cultures (25).

As proposed for denitrifying bacteria (21, 22, 30), the initial step in the degradation of phthalate isomers is suggested to be decarboxylation to benzoate because (i) all the phthalate-isomer-grown cultures were capable of benzoate degradation without a lag phase and (ii) small amounts of benzoate accumulated in phthalate-isomer-degrading cultures incubated with the methanogenic inhibitor BES.

Modelling degradation of the phthalate isomers and benzoate. In order to describe the dynamic formation and consumption of acetate and hydrogen during degradation of the phthalate isomers and benzoate, a mathematical model was developed (see Appendix). The model was based on the reaction stoichiometries shown in Table 1. Even though no shift in microbial population can be excluded to occur during benzoate degradation, we assumed that one organism was responsible for the fermentation of the phthalate isomers and benzoate. Additional kinetic parameter values that were required as input for the model were calculated using equations 3 to 5.

The calculated biomass yields of the phthalate- and benzoate-fermenting organisms (equation 3) are presented in Table 3. For the biomass yield of the acetoclastic methanogens in the mixed culture, the measured values as reported in Table 2 were used. For the biomass yield of the hydrogenotrophic methanogens we estimated a value of $0.33 \text{ g} \cdot \text{mol-H}_2^{-1}$ from the energetic efficiency for growth under hydrogen-limiting conditions of *Methanobacterium bryantii* (27). With this estimated value, the maximum contribution of the biomass yield of the hydrogenotrophic methanogens to the total biomass yield during growth on the phthalate isomers or benzoate amounts to only 12%, suggesting that the errors introduced into the calculations of the biomass yield of the fermenting organisms are small.

Based on measured values for the maximum specific growth rate on the phthalate isomers and benzoate (Table 2) and the corresponding biomass yield values of the fermenting bacteria (Table 3), the maximum specific conversion rates for benzoate and the phthalate isomers ($q_{\text{XFermS}}^{\text{max}}$) were calculated (Table 3).

The results indicate that the maximum specific conversion rates for benzoate and the phthalate isomers are in the same order of magnitude, which confirms the observation that the initial rates of degradation of benzoate and the phthalate isomers are comparable, as described above.

The observation that acetate and hydrogen concentrations remained constant during degradation of the phthalate isomers allowed for calculation of (i) the biomass concentration ratios $C_{\text{XFerm}}/C_{\text{XAcM}}$ and $C_{\text{XFerm}}/C_{\text{XHyM}}$ according to equation 4 and (ii) the half-saturation constants for the methanogenic substrates acetate and hydrogen (K_{C_2} and K_{H_2}) according to Equation 5. To enable calculation of K_{H_2} , we estimated from the data reported by Seitz et al. (27) a value of $0.60 \text{ mol-H}_2 \cdot \text{g}^{-1} \cdot \text{day}^{-1}$ for $q_{\text{H}_2}^{\text{max}}$. Calculated values for these parameters are shown in Table 4.

By using the measured and estimated parameter values (shown in Tables 2 to 4), the degradation of the phthalate isomers and benzoate can be described with the initial concentration of fermenting bacteria $[X_{\text{XFerm}}(0)]$ as the only variable (and estimated values for K_{BA} and K_{PA}). When the boundary conditions are sufficiently fulfilled, the derived model accurately describes the accumulation of acetate and hydrogen during the degradation of the phthalate isomers, as shown for terephthalate degradation in Fig. 2.

The assumptions made to calculate the biomass ratios and the half-saturation constants for the methanogens (Table 4) were based on measurements with the phthalate isomers as a substrate. To validate the model, intermediate accumulation and product formation during benzoate degradation were calculated. From the results shown in Fig. 4 it can be seen that the intermediate formation of acetate and final production of methane are reasonably well predicted for benzoate degradation. If it is taken into account that minor errors in, for ex-

TABLE 4. Calculated specific biomass ratios and apparent half-saturation constants for acetate and hydrogen for the methanogens in the phthalate-isomer-degrading mixed cultures

Culture	$\frac{X_{\text{XFerm}}}{X_{\text{AcM}}}$ (g · g ⁻¹)	$\frac{X_{\text{XFerm}}}{X_{\text{HyM}}}$ (g · g ⁻¹)	K_{C_2} (mM)	K_{H_2} (Pa)
Isophthalate	1.7	4.9	0.7	4.0
ortho-Phthalate	1.5	4.4	0.6	5.1
Terephthalate	1.1	4.2	0.4	3.4

ample, the measured values for $Y_{X_{AcM}C_2}$ lead to large differences in the estimated biomass ratio, the results are satisfactory.

In summary, we suggest that the developed three-species model adequately describes the intermediate accumulation of acetate and hydrogen and the final production of methane during degradation of the phthalate isomers and benzoate. Description of the conversions observed as a function of the kinetic properties of the individual trophic groups in the mixed culture provides additional insight into its metabolic properties.

Kinetic parameter values. Measured and estimated values of the kinetic parameters for benzoate and acetate degradation correspond well with previously reported values. A growth yield on benzoate of $8.5 \text{ g} \cdot \text{mol-benzoate}^{-1}$ has been reported for strain BZ-2 cocultured with *Methanospirillum* sp. strain PM-1 (assuming a protein content of 60%) (6) and of 6.2 and $8.2 \text{ g} \cdot \text{mol-benzoate}^{-1}$ for *Syntrophus buswellii* GA cocultured with *Methanospirillum hungatei* or *Desulfovibrio* sp., respectively (1). From our data we calculated a similar average value of $9.3 \pm 0.5 \text{ g} \cdot \text{mol-benzoate}^{-1}$ if the growth of acetoclastic methanogens was omitted from the calculation.

Maximum specific growth rates reported for two different *Syntrophus buswellii* strains, cocultured with either *M. hungatei* or *Desulfovibrio* sp., are 0.10 to 0.29 and 0.17 to 0.37 day^{-1} , respectively (19, 32). The average value of $0.17 \pm 0.04 \text{ day}^{-1}$ we obtained for the maximum growth rate on benzoate in our cultures is in the same order of magnitude.

Methanosaeta-like organisms were observed in all three phthalate isomers degrading mixed cultures by microscopical observation. The biomass yield, half-saturation constant, and maximum growth rate reported in the literature for *Methanosaeta soehngenii* grown on acetate at 37°C are $1.47 \text{ g} \cdot \text{mol-acetate}^{-1}$, 0.47 mM, and 0.11 day^{-1} , respectively (33). These values are in the same order of magnitude as the average values we measured or calculated for our cultures ($Y_{XC_2} = 1.15 \pm 0.28 \text{ g} \cdot \text{mol-acetate}^{-1}$, $K_{C_2} = 0.55 \pm 0.13 \text{ mM}$ and $\mu_{C_2}^{\text{max}} = 0.12 \pm 0.02 \text{ day}^{-1}$).

In the literature no kinetic parameter values for methanogenic cultures degrading one of the phthalate isomers were found. The maximum growth rates we calculated for the phthalate isomers (μ_{PA}^{max}) were low: $0.091 \pm 0.003 \text{ day}^{-1}$. Comparable values have been found for methanogenic enrichment cultures degrading the poorly degradable substrates toluene and *ortho*-xylene (0.11 and 0.07 day^{-1} , respectively [7]).

Energetic efficiency for growth on the phthalate isomers and benzoate. Correlations between thermodynamics and biomass yields have been developed by several researchers (11, 17, 29). Stouthamer (29) stated that the biomass yield of anaerobic bacteria is in the range of 5 to $12 \text{ g} \cdot \text{mol-ATP}^{-1}$, with an average value of $10.5 \text{ g} \cdot \text{mol-ATP}^{-1}$. Under physiological conditions, an average amount of $70 \text{ kJ} \cdot \text{mol-ATP}^{-1}$ was estimated to be needed for irreversible ATP synthesis (25). With average values for the substrate and product concentrations for fermentation of the phthalate isomers and benzoate, the Gibbs free energy change of the fermentations and the biomass yield normalized to an energy quantum of $70 \text{ kJ} \cdot \text{mol}^{-1}$ ($Y_{X_{Ferm}\Delta G}$) can be calculated from the measured specific biomass yields ($Y_{X_{Ferm,S}}$), as shown in Table 3.

The average value we calculated for $Y_{X_{Ferm}\Delta G}$ for benzoate fermentation is $11.2 \pm 1.9 \text{ g} \cdot 70\text{-kJ}^{-1}$, which is close to the average value of $10.5 \text{ g} \cdot \text{mol-ATP}^{-1}$ reported by Stouthamer (29). Values for $Y_{X_{Ferm}\Delta G}$ for fermentation of the phthalate isomers are much lower ($3.3 \pm 0.3 \text{ g} \cdot 70\text{-kJ}^{-1}$), suggesting that the energetic efficiency for growth on the phthalate isomers is much lower compared to benzoate. The observation that no degradation of the phthalate isomers was observed at Gibbs

free-energy changes exceeding $-65 \text{ kJ} \cdot \text{mol}^{-1}$ confirms that an energetic inefficiency in degradation of the phthalate isomers may exist. Assuming that the phthalate isomers and benzoate are degraded by the same organism and that benzoate is the first intermediate in the degradation of the phthalate isomers, the postulated energetic inefficiency during growth on the phthalate isomers should manifest within the initial steps of the phthalate isomer degradation.

A possible reason for the postulated energetic inefficiency in fermentation of the phthalate isomers can be found in the mechanism of substrate transport across the microbial membrane. The $\text{pK}_{a1,2}$ values for the phthalate isomers ($\text{pK}_{a1,2}$ for *ortho*-, *iso*-, and *terephthalate* are 3.0, 3.6, and 3.5, respectively) are considerably lower than the pK_a value of 4.2 for benzoate (8). To enable comparable uptake rates for the phthalate isomers and benzoate as suggested by the comparable values for $q_{X_{Ferm,PA}}^{\text{max}}$ and $q_{X_{Ferm,BA}}^{\text{max}}$ (Table 3), active uptake under expense of Gibbs free-energy may be required for the phthalate isomers, whereas no (or less) energy is required for the uptake of benzoate.

Another explanation for the postulated energetic inefficiency can be found in the decarboxylation of the phthalates to benzoate (or their CoA analogues). Taylor and Ribbons (30) suggested that decarboxylation of phthalate may proceed after the initial partial reduction of the aromatic ring (in a one- or two-electron mechanism), followed by oxidative decarboxylation. The initial reduction of the aromatic ring is endergonic and requires the investment of energy in the form of ATP (3). If this amount of energy cannot (or can only partially) be regained during oxidative decarboxylation, this may explain the net energy consumption during decarboxylation of the phthalate isomers.

In summary, it is postulated that the calculated low energetic efficiency for growth on the phthalate isomers can be due to the need for energy consumption (i) for active uptake of the phthalate isomers across the microbial membrane or (ii) to initiate the decarboxylation of the phthalate isomers to benzoate.

ACKNOWLEDGMENTS

We thank A. E. van Aelst and G. Gonzalez for help with electron microscopy. R.K. wishes to thank Hervé Macarie and Alfons J. M. Stams for critical review of the manuscript.

This project was supported through IOP Milieubiotechnologie (Innovative Research Program Environmental Biotechnology, The Hague, The Netherlands).

APPENDIX

A mathematical model was developed for predicting the intermediate accumulation of acetate and hydrogen and for production of methane during degradation of the phthalate isomers and benzoate. The model is based on Monod kinetics (18) and, consequently, the volumetric rate of substrate consumption (A-1), biomass growth (A-2), and product formation (A-3) in a batch reactor can be described by using the following equations (neglecting maintenance and/or decay):

$$R_S = -\frac{\mu_S^{\text{max}}}{Y_{XS}} \cdot \frac{C_S}{K_S + C_S} \cdot C_X \quad (\text{A-1})$$

$$R_X = -Y_{XS} \cdot R_S \quad (\text{A-2})$$

$$R_P = -f_{SP} \cdot (1 - \eta_{XS}) \cdot R_S \quad (\text{A-3})$$

where f_{SP} stands for the number of moles of product formed per mole of substrate according to the chemical reaction equation $\text{mol-S} \cdot \text{mol-P}^{-1}$ and where η_{XS} is the biomass yield for growth of biomass X on substrate S, expressed as electron yield ($\text{e-mol-X} \cdot \text{e-mol-S}^{-1}$). This parameter can be calculated from the measured (or calculated) biomass yield according to the following equation:

$$\begin{aligned} \frac{dC_{PA}}{dt} &= R_{PA} & \text{A-5} \\ \frac{dC_{BA}}{dt} &= R_{BA} & \text{A-6} \\ \frac{dC_{C2}}{dt} &= -f_{BAC2} \cdot (1 - \eta_{X_{Ferm}BA}) \cdot R_{BA} - f_{PAC2} \cdot (1 - \eta_{X_{Ferm}PA}) \cdot R_{PA} + R_{C2} & \text{A-7} \\ \frac{dC_{H2}}{dt} &= \left\{ \begin{array}{l} -f_{BAH2} \cdot (1 - \eta_{X_{Ferm}BA}) \cdot R_{BA} - f_{PAH2} \cdot \\ (1 - \eta_{X_{Ferm}PA}) \cdot R_{PA} + R_{H2} \cdot (1 - \exp(\Delta G_{H2ox}/R \cdot T)) \end{array} \right\} \cdot \frac{V_g}{V_{liquid}} \cdot V_{mg} & \text{A-8} \\ \frac{dC_{CH4}}{dt} &= -f_{H2CH4} \cdot (1 - \eta_{X_{HyM}H2}) \cdot R_{H2} - f_{C2CH4} (1 - \eta_{X_{AcM}C2}) \cdot R_{C2} & \text{A-9} \\ \frac{dC_{X_{Ferm}}}{dt} &= -Y_{X_{Ferm}BA} \cdot R_{BA} - Y_{X_{Ferm}PA} \cdot R_{PA} & \text{A-10} \\ \frac{dC_{X_{AcM}}}{dt} &= -Y_{X_{AcM}C2} \cdot R_{C2} & \text{A-11} \\ \frac{dC_{X_{HyM}}}{dt} &= -Y_{X_{HyM}H2} \cdot R_{H2} & \text{A-12} \end{aligned}$$

FIG. A1. Differential equations describing terephthalate and benzoate degradation with concomitant production and consumption of acetate and hydrogen and production of methane.

$$\eta_{xs} = \frac{\gamma_x \cdot C \cdot \text{length}_x}{\gamma_s \cdot C \cdot \text{length}_s \cdot MW_x} \cdot Y_{xs} \quad (\text{A-4})$$

where γ is the degree of reduction (e-mol · C-mol⁻¹) as defined by Heijnen et al. (11), C-length is the carbon chain length (C-mol · mol⁻¹), and MW is the molecular weight (g · mol⁻¹). We used an average biomass composition of C₄H_{7.2}O₂N_{0.8} (11, 16) and NH₄⁺ as the nitrogen source. By using these kinetic equations and mass balances based on the stoichiometry of the conversion reactions shown in Table 1, differential equations for all substrates, products, and different types of biomass were derived (Fig. A1). During the derivation of these equations the following assumptions were made: (i) the phthalate isomers and benzoate are fermented by the same organism (X_{Ferm}); (ii) kinetic parameters for fermentation of the phthalate isomers and benzoate may be different; and (iii) the ratio of fermentation products equals the ratio predicted by the chemical conversion reactions described in Table 1 and is therefore independent of biomass growth.

The differential equation describing the change in hydrogen concentration over time is expressed in atm · (liter · day)⁻¹ by correction of the molar rates for the liquid volume (V_{liquid}, liter), the headspace volume (V_g, liter), of the serum bottle, and the volume of 1 mole of gas (V_{mg}, liter · mol⁻¹). To include the observed threshold concentrations of hydrogen in the model, an additional term was included in the differentialequationdescribinghydrogenconsumptionduetohydrogenotrophic methanogenesis. This term is based on reversible enzyme kinetics as described by Labib et al. (15) and avoids hydrogen consumption if hydrogenotrophic methanogenesis is endergonic ($\Delta G'_{H2ox} > 0$). No product inhibition terms for the fermentation of the phthalate isomers and benzoate were included in the model because in general only small amounts of acetate and hydrogen accumulated during our experiments.

The differential equations A-5 to A-12 (Fig. A1) were integrated by using a fourth-order Runge-Kutta algorithm with adaptive step-size control (24). Optimization of parameter values or initial conditions was performed by using the downhill simplex method in multi-dimensions as described by Press et al. (24). Optimization was based on minimizing the absolute error between measured and calculated values for the individual concentrations. The software program incorporating the model was written in Turbo Pascal 6.0 on a personal computer (80486-DX33).

An example of the model is shown in Fig. A2 for the degradation of

terephthalate and benzoate. This figure clearly demonstrates the differences in intermediate accumulation during terephthalate and benzoate degradation. The parameter values used for calculating Fig. A2 are presented in Tables 2 to 4.

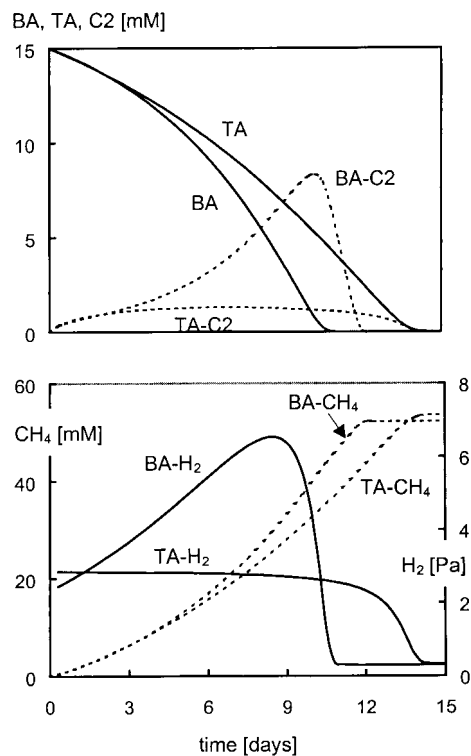


FIG. A2. Terephthalate (TA) and benzoate (BA) degradation and concomitant intermediate accumulation of acetate (C2) and hydrogen (H₂) and final production of methane (CH₄) as predicted by the model.

REFERENCES

1. **Auburger, G., and J. Winter.** 1995. Isolation and physiological characterization of *Syntrophus buswellii* strain GA from a syntrophic benzoate-degrading, strictly anaerobic coculture. *Appl. Microbiol. Biotechnol.* **44**:241–248.
2. **Bemis, A. G., J. A. Dindorf, B. Horwood, and C. Samans.** 1982. Phthalic acids and other benzenepolycarboxylic acids, p. 732–777. *In* H. F. Mark, D. F. Othmer, C. G. Overberg, G. T. Seaborg, M. Grayson, and D. Eckroth (ed.), *Kirk Othmer encyclopedia of chemical technology*, vol. 17. John Wiley & Sons, New York, N.Y.
3. **Boll, M., and G. Fuchs.** 1995. Benzoyl-coenzyme A reductase (dearomatizing), a key enzyme of anaerobic aromatic metabolism. ATP dependence of the reaction, purification and some properties of the enzyme from *Thauera aromatica* strain K172. *Eur. J. Biochem.* **234**:921–933.
4. **Conrad, R., and B. Wetter.** 1990. Influence of temperature on energetics of hydrogen metabolism in homoacetogenic, methanogenic, and other bacteria. *Arch. Microbiol.* **155**:94–98.
5. **Dimroth, K.** 1983. Thermochemische daten organischer verbindungen, p. 997–1038. *D'ans-Lax, Taschenbuch für chemiker und Physiker*, vol. 2. Springer-Verlag, Berlin, Germany.
6. **Dolfing, J., and J. M. Tiedje.** 1988. Acetate inhibition of methanogenic, syntrophic benzoate degradation. *Appl. Environ. Microbiol.* **54**:1871–1873.
7. **Edwards, E. A., and D. Grbic-Galic.** 1994. Anaerobic degradation of toluene and *o*-xylene by a methanogenic consortium. *Appl. Environ. Microbiol.* **60**:313–322.
8. **Fieser, L. F., and M. Fieser.** 1956. *Organic chemistry*, 3rd ed. Reinhold Publishing Corp., New York, N.Y.
9. **Fuchs, G., M. E. S. Mohamed, U. Altenschmidt, J. Koch, A. Lack, R. Brackmann, C. Lochmeyer, and B. Oswald.** 1994. Biochemistry of anaerobic biodegradation of aromatic compounds, p. 513–553. *In* C. Ratledge (ed.), *Biochemistry of microbial degradation*. Kluwer Academic Publishers, Dordrecht, The Netherlands.
10. **Giam, C. S., E. Atlas, M. A. Powers, Jr., and J. E. Leonard.** 1984. Phthalic acid esters, p. 67–140. *In* O. Hutzinger (ed.), *Anthropogenic compounds*, vol. 3, part C. Springer-Verlag, Berlin, Germany.
11. **Heijnen, J. J., M. C. M. van Loosdrecht, and L. Tijhuis.** 1992. A black box mathematical model to calculate auto- and heterotrophic biomass yields based on Gibbs energy dissipation. *Biotechnol. Bioeng.* **40**:1139–1154.
12. **Huser, B. A., K. Wuhrmann, and A. B. J. Zehnder.** 1980. *Methanotherix soehngenii* gen. nov. sp. nov., a new acetotrophic non-hydrogen-oxidizing methane bacterium. *Arch. Microbiol.* **132**:1–9.
13. **Kleerebezem, R., L. W. Hulshoff Pol, and G. Lettinga.** Anaerobic biodegradability of aromatic acids and esters. *Biodegradation*, in press.
14. **Kleerebezem, R., L. W. Hulshoff Pol, and G. Lettinga.** 1999. The role of benzoate in anaerobic degradation of terephthalate. *Appl. Environ. Microbiol.* **65**:1161–1167.
15. **Labib, F., J. F. Ferguson, M. M. Benjamin, M. Merigh, and N. L. Ricker.** 1993. Mathematical modelling of an anaerobic butyrate degrading consortium: predicting their response to organic overloading. *Environ. Sci. Technol.* **27**:2673–2683.
16. **McCarty, P. L.** 1971. Energetics and bacterial growth, p. 495–512. *In* S. D. Faust and J. V. Hunter (ed.), *Organic compounds in aquatic environments*. Marcel Dekker, Inc., New York, N.Y.
17. **McCarty, P. L.** 1972. Energetics of organic matter degradation, p. 91–118. *In* R. Mitchell (ed.), *Water pollution microbiology*. John Wiley & Sons, New York, N.Y.
18. **Monod, J.** 1949. The growth of bacterial cultures. *Annu. Rev. Microbiol.* **3**:371–394.
19. **Mountfort, D. O., W. J. Brulla, L. R. Krumholz, and M. P. Bryant.** 1984. *Syntrophus buswellii* gen. nov., sp. nov.: a benzoate catabolizer from methanogenic ecosystems. *Int. J. Syst. Bacteriol.* **34**:216–217.
20. **Naumov, A. V., A. B. Gafarov, and A. M. Boronin.** 1996. A novel *ortho*-phthalate utilizer—an acetic acid bacterium *Acetobacter* sp. *Microbiology* **65**:182–186.
21. **Nozawa, T., and Y. Maruyama.** 1988. Anaerobic metabolism of phthalate and other aromatic compounds by a denitrifying bacterium. *J. Bacteriol.* **170**:5778–5784.
22. **Nozawa, T., and Y. Maruyama.** 1988. Denitrification by a soil bacterium with phthalate and aromatic compounds as substrates. *J. Bacteriol.* **170**:2501–2505.
23. **Powell, G. E.** 1984. Equalisation of specific growth rates for syntrophic associations in batch cultures. *J. Chem. Technol. Biotechnol.* **34B**:97–100.
24. **Press, W. H., B. P. Flannery, S. A. Teukolsky, and W. T. Vetterling.** 1989. *Numerical recipes in Pascal: the art of scientific computing*. Cambridge University Press, Cambridge, United Kingdom.
25. **Schink, B.** 1992. Syntrophism among prokaryotes, p. 276–299. *In* A. Balows, H. G. Trüper, M. Dworkin, W. Harder, and K. H. Schleifer (ed.), *The prokaryotes*, vol. 1. Springer-Verlag, New York, N.Y.
26. **Schink, B., A. Brune, and S. Schnell.** 1992. Anaerobic degradation of aromatic compounds, p. 219–242. *In* G. Winkelmann (ed.), *Microbial degradation of natural products*. VCH, Weinheim, Germany.
27. **Seitz, H. J., B. Schink, N. Pfennig, and R. Conrad.** 1990. Energetics of syntrophic ethanol oxidation in defined chemostat cocultures: energy sharing in biomass production (2). *Arch. Microbiol.* **155**:89–93.
28. **Stams, A. J. M.** 1994. Metabolic interactions between anaerobic bacteria in methanogenic environments. *Antonie Leeuwenhoek* **66**:271–294.
29. **Stouthamer, A. H.** 1979. The search for correlation between theoretical and experimental growth yields. *Int. Rev. Biochem.* **21**:1–47.
30. **Taylor, B. F., and D. W. Ribbons.** 1983. Bacterial decarboxylation of *o*-phthalic acids. *Appl. Environ. Microbiol.* **46**:1276–1281.
31. **Thauer, R. K., K. Jungermann, and K. Decker.** 1977. Energy conservation in chemotrophic anaerobic bacteria. *Bacteriol. Rev.* **41**:100–179.
32. **Wallrabenstein, C., and B. Schink.** 1994. Evidence of reversed electron transport in syntrophic butyrate or benzoate oxidation by *Syntrophomonas wolfei* and *Syntrophus buswellii*. *Arch. Microbiol.* **162**:136–142.
33. **Zehnder, J. B., B. A. Huser, T. D. Brock, and K. Wuhrmann.** 1980. Characterization of an acetate-decarboxylating, non-hydrogen-oxidizing methane bacterium. *Arch. Microbiol.* **124**:1–11.